Downloaded from orbit.dtu.dk on: May 04, 2023

DTU Library

Effects of surface design on aerodynamic forces of iced bridge cables

Koss, Holger

Published in:
Proceedings of the Symposium on the Dynamics and Aerodynamics of cables

Publication date:
2014

Document Version
Peer reviewed version

Link back to DTU Orbit

Citation (APA):
Koss, H. (2014). Effects of surface design on aerodynamic forces of iced bridge cables. In *Proceedings of the Symposium on the Dynamics and Aerodynamics of cables*

General rights
Copyright and moral rights for the publications made accessible in the public portal are retained by the authors and/or other copyright owners and it is a condition of accessing publications that users recognise and abide by the legal requirements associated with these rights.

- Users may download and print one copy of any publication from the public portal for the purpose of private study or research.
- You may not further distribute the material or use it for any profit-making activity or commercial gain
- You may freely distribute the URL identifying the publication in the public portal

If you believe that this document breaches copyright please contact us providing details, and we will remove access to the work immediately and investigate your claim.

EFFECT OF SURFACE DESIGN ON AERODYNAMIC FORCES OF ICED BRIDGE CABLES

Holger HUNDBORG KOSS
Technical University of Denmark – Brovej, Building 118, 2800 Kgs. Lyngby – Denmark
hko@byg.dtu.dk

Introduction

In recent years the relevance of ice accretion for wind-induced vibration of structural bridge cables has been recognised and became a subject of research in bridge engineering. Full-scale monitoring and observation indicate that light precipitation at moderate low temperatures between zero and -5°C may lead to large amplitude vibrations of bridge cables under wind action. For the prediction of aerodynamic instability quasi-steady models have been developed estimating the cable response magnitude based on structural properties and aerodynamic force coefficients for drag, lift and torsion. The determination of these force coefficients require a proper simulation of the ice layer occurring under the specific climatic conditions, favouring real ice accretion over simplified artificial reproduction. The work presented in this paper was performed to study whether the design of bridge cable surface influences the accretion of ice to an extent that the aerodynamic forces differ significantly amongst the designs. The experiments were conducted in a wind tunnel facility capable amongst others to simulate in-cloud icing conditions.

TESTED BRIDGE CABLE TUBES

Designs

The study of ice accretion effects on the cable aerodynamics was performed on the same tube types as used and described by Kleissl and Georgakis in [1]: (a) a plain HDPE tube, (b) a HDPE tube fitted with helical fillets and (c) a HDPE tube with a pattern-indented surface (Figure 1).

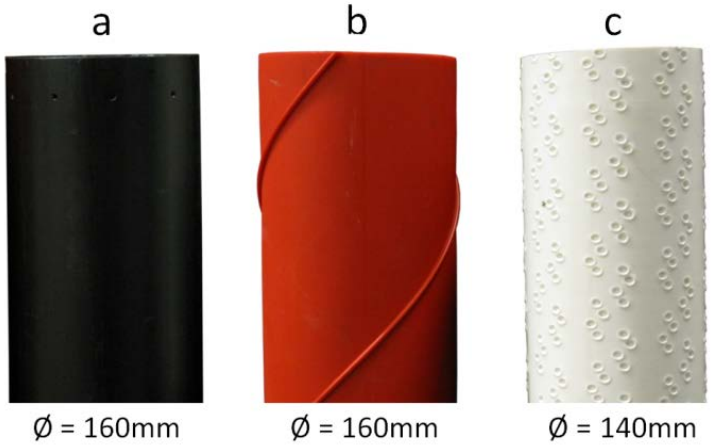

Figure 1 Bridge cable cover tubes tested in the ice accretion study: (a) a plain HDPE tube, (b) tube wrapped with two helical fillets, (c) a tube with a pattern-indented surface texture.

The sectional models are original full-scale samples. The plain HDPE tube has 160mm outer diameter and a measured average surface roughness of $R_a \approx 1.8\mu m$ [2]. The HDPE tube with two helically wrapped fillets has an outer diameter of 160mm as well. The fillets are rounded with a height of approximately 3mm and a base width of approximately 4mm. Furthermore, they have a 3.14 tube diameter pitch length (502mm and 45°). The average material surface roughness is in the order of R_a

≈ 3.0µm. The pattern-indented tube has a diameter of 140mm, and is an actual sample of the most common diameter of cable used on the Sutong Bridge. The relative surface roughness is defined by the depth of the indentations, measured to be approximately 1% of cable diameter. The relevance of using original cover tubes instead of recreations is documented in studies focusing on the influence of surface roughness and non-circularity on aerodynamic force coefficients [2]. Especially the lift coefficient is sensible to surface roughness irregularities and cross-sectional distortion.

Reference Aerodynamic Performance

The aerodynamic performance of the three cable tubes shown in Figure 1 have been studied and reported in [1]. Figure 2 (left) shows the development of the drag force coefficient, C_D, over Reynolds number and the lift coefficients (to the right), C_L, for the three cable types as shown in Figure 1. As discussed in [2] the lift force on the plain cable tube is very susceptible to surface roughness and the measured results vary significantly on the angle of attack, α, even for wind normal to cable axis (cross-flow condition).

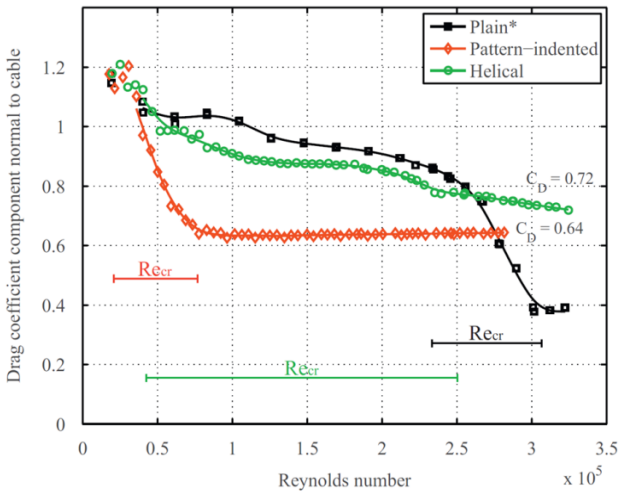

Drag force coefficient, C_D, as function of Reynolds number for the three cable types in dry condition and flow normal to cable axis. For each cable type the corresponding critical range of significant drag force reduction is indicated [1].

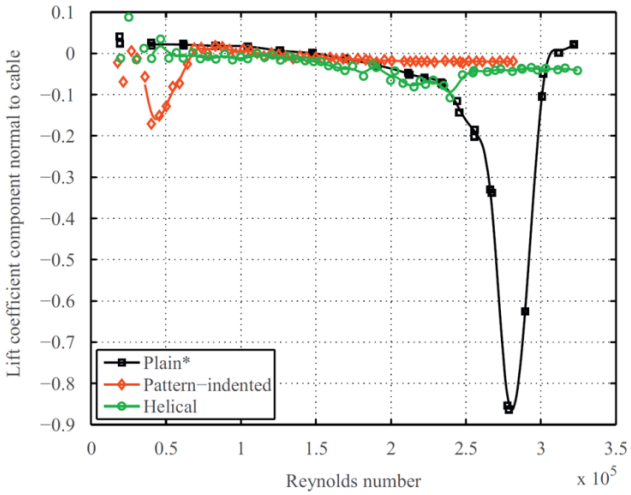

Lift coefficient, C_L, as function of Reynolds number for the three cable types in dry condition and flow normal to cable axis [1].

Figure 2 Reference aerodynamic performance (Maximum turbulence intensity $I_{u,max}$ = 0.6%).

EXPERIMENTAL SETUP & TEST CONDITIONS

The tests were performed in the collaborative Climatic Wind Tunnel (CWT) at FORCE Technology in Lyngby, Denmark. The wind tunnel was developed and built between 2008 and 2010 as a joint project between the Technical University of Denmark (DTU), FORCE Technology funded by the Danish bridge owners/operators Femmern Bælt A/S and Storebælt A/S. The main technical specifications are: 5m long test chamber with a cross-section of 2 x 2m, maximum airspeed u_{max} = 32m/s, lowest turbulence intensity is $I_{u,min}$ = 0.6%. The lowest long-term average temperature at full speed is -4.5°C. The blockage ratio for a 160mm diameter cable segment is about 8%. Further information is available in [3]. Heart of the CWT is the cooling system capable of operating the facility at sub-zero air temperatures and the developed spray system allows for creation of in-cloud icing conditions. The spray bar is equipped with 15 nozzles producing droplets in the size range between 10 and 80µm (median volume diameter, *MVD*) depending on the air/water pressure ratio and magnitude. The spray bar can be rotated steplessly to assume any position for testing inclined cables ([4], [5], [6]).

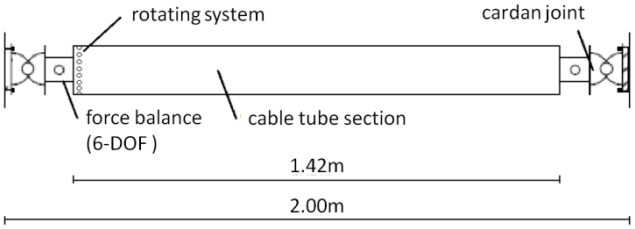

Arrangement for force measurement in the middle of the test section to capture the aerodynamic loads for varying airspeed and rotation angle α.

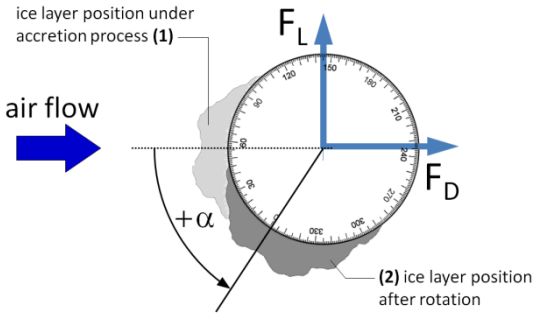

Orientation of drag and lift forces. The angle of rotation α (counter-clockwise) corresponds to the clockwise relative angle of attack.

Figure 3 Force measurement setup and definition of ice layer position.

Figure 3 (left) illustrates the arrangement of the cable test specimen, the two 6-component AMTI MC3A-500 force balances on each side of the cable and the joint connections to the wind tunnel walls to avoid end-moment effects. The cable tube can be rotated in steps of $\Delta\alpha = 10°$ around its length axis. The corresponding lift and drag force coordinate system is shown to the right in Figure 3. The position of the ice layer is measured in degrees as the angular distance between its location during accretion (1) and the location during wind load testing (2) counting positive for counter-clockwise rotation. In 2009 a fundamental study on ice accretion on circular cylinders at moderate low temperatures was performed at the National Research Counsil (NRC) in Ottawa, Canada [7]. 'Moderate low temperatures' refer to air temperatures between 0 and -5°C at which ice accretion and subsequent large amplitude wind-induced vibrations have been observed on bridges in the past. This temperature range can be divided into three sub-ranges: high moderate temperatures (0 to -2°C) characterised by wet ice accretion (glaze), low moderate (-3 to -5°C) with dry ice (rime) and a transition range around -3°C with a mixed ice type. In this study ice accretion in the high and low temperature range has been simulated with target temperatures of -2 and -5°C for wet and dry ice, respectively. Table 1 summarises the boundary conditions of the simulations including the measured ice mass after 60 minutes of accretion. The airspeed during icing was u = 10.5m/s with a maximum along-wind turbulence intensity of I_u = 0.6%.

TABLE 1Simulation Conditions: Settings and Achieved Values

cable tube type	**icing condition**	**ID** [-]	**mean air temp.** [°C]	**accretion time** [min]	**MVD**[1] [µm]	**LWC**[2] [g/m³]	**ice mass** [kg/m]
a) standard plain	wet	SW	-2.0	60	10-15	0.4	0.60
	dry	SD	-5.1	60	10-15	0.4	0.56
b) helical fillet	wet	HW	-2.2	60	10-15	0.4	0.46
	dry	HD	-5.1	60	10-15	0.4	0.49
c) pattern-indented	wet	PW	-1.8	60	10-15	0.4	0.53
	dry	PD	-5.3	60	10-15	0.4	0.60

[1] The MVD is estimated based on nozzle specification provided by the manufacturer using the air/water pressure ratio and magnitude.
[2] The LWC of 0.4g/m³ is a target value. Comparison tests indicate that the true value might be higher by 30%.

Even though untypical for bridge cables the tube specimens were mounted horizontally for comparison with the observation data base from the NRC tests regarding the ice accretion characteristics [7]. Furthermore, the orientation allowed for easy dynamic testing of galloping instability in a simple free vibration setup for vertical cross-flow vibrations [4].

CONSIDERATIONS FOR EVALUATION

An ice layer perfectly symmetric around the stagnation point during the accretion process will be reflected by a symmetric drag force curve $C_D(\alpha)$ and an antisymmetric lift force curve $C_L(\alpha)$. Influence on the symmetry can be expected from gravity effects on the droplets during the accretion process – in particular for wet ice accretion. The influence of gravity on the aerodynamic forces is indicated in the graphs by mirroring the main characteristic of the force curve functions assuming a minimum level of symmetry. The offset Θ (measured in degrees) of the force symmetry point from the flow stagnation point gives an indication of the magnitude of the gravity effect on the ice accretion. The mirrored force functions are displayed as a dotted line in the graphs.

RESULTS

Standard Plain Cable

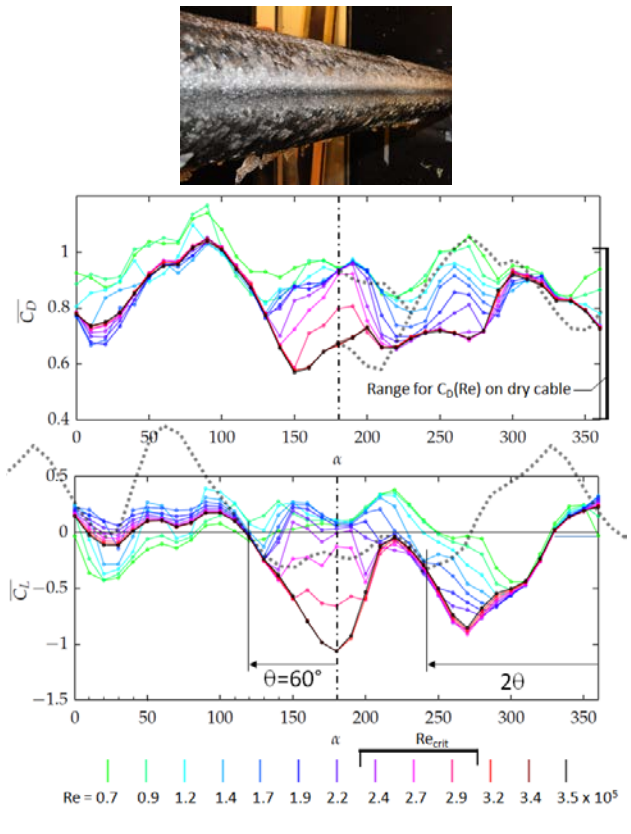

Wet ice accretion (Accretion time: 60min; mean air temperature: -2°C; ice mass: 0.6kg/m).

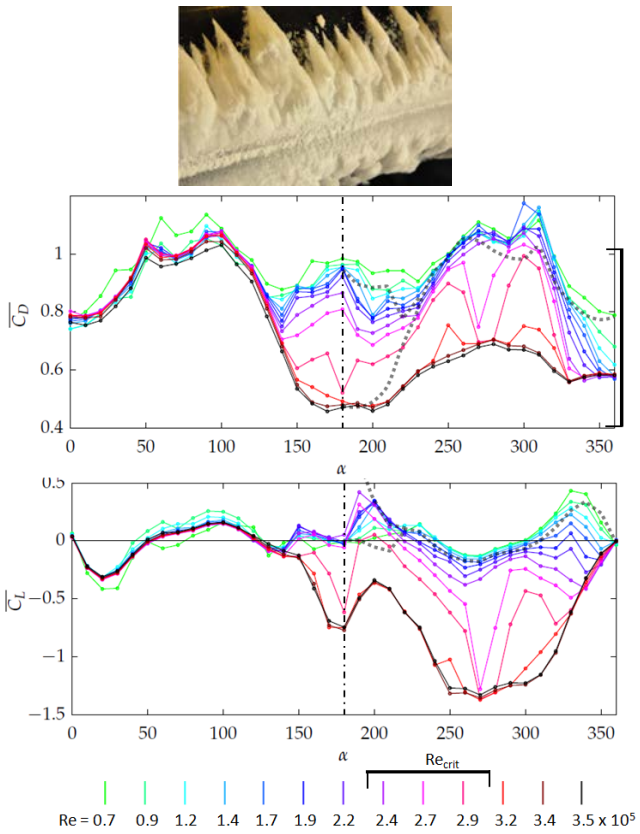

Dry ice accretion (Accretion time: 60min; mean air temperature: -5.1°C; ice mass: 0.56kg/m).

Figure 4 Drag and lift coefficients of standard plain cable tube.

For wet ice accretion the ice layer exhibits a high irregularity hence the antisymmetric image of the lift curve matches the measured data only in few features. The resulting dominant angle for neutral lift at $\alpha = 120°$, i.e. from rear below. The poor match in the lift curves indicates that gravity influences the wet ice accretion on the plain standard cable significantly. The high irregularity affects the drag force as well. Expecting a curve mirrored around $\alpha = 180°$ (grey dotted line) only a vague resemblance between both sides can be observed. For some angles of attack the drag force of the iced plain cable still exhibits a Reynolds dependency as measured on the dry cable (Figure 2, left). For other angles the dependency of C_D almost disappears. With the ice layer near the flow separation points the cable

assumes a sharp-edged body characteristic. It seems that the ranges of flow angles with a high Reynolds dependency of C_D are similar to those where C_L varies with Reynolds number as well. In Figure 4 (left) the range for the drag coefficient measured on the dry cable (right graph border) and the corresponding critical Reynolds range are indicated for comparison purpose. Around $\alpha = 180°$ the critical Reynolds range of the iced cable is similar to the dry cable. As one could expect, the drag coefficient is generally higher on the iced cable but stays largely within the drag range of the dry cable.

For dry ice accretion (Figure 4, right) the ice layer is more concentrated around the stagnation line on the upstream side of the cable tube. For up to $\alpha = 120°$ the drag force is little affected by the Reynolds number indicating a rather sharp-edged body behaviour than of a circular cylinder. Between 120° and 180° the drag force is strongly dependent on Re. Here, the ice layer is fully immersed in the separated wake flow on the rear side of the cable and the tube appears aerodynamically similar to a dry cylinder with the characteristic critical Reynolds regime. Around 180° the drag coefficient C_D is quite symmetric. This symmetry however does not extend to flow direction beyond 210°, where, according to observations below 120°, the drag force should become again independent of Reynolds number. A reason for this asymmetry of $C_D(\alpha)$ is a change in the surface roughness during the course of testing. Under dry ice accretion simulation fine spray dust creates small ice flake accumulation on the rear side of the cable surface. These flakes get blown off at higher airspeeds when directly exposed to the approaching wind. As a consequence the surface roughness is changed in the second half of the tests clearly affecting the Reynolds dependency for both drag and lift force.

Helical Fillet Cable

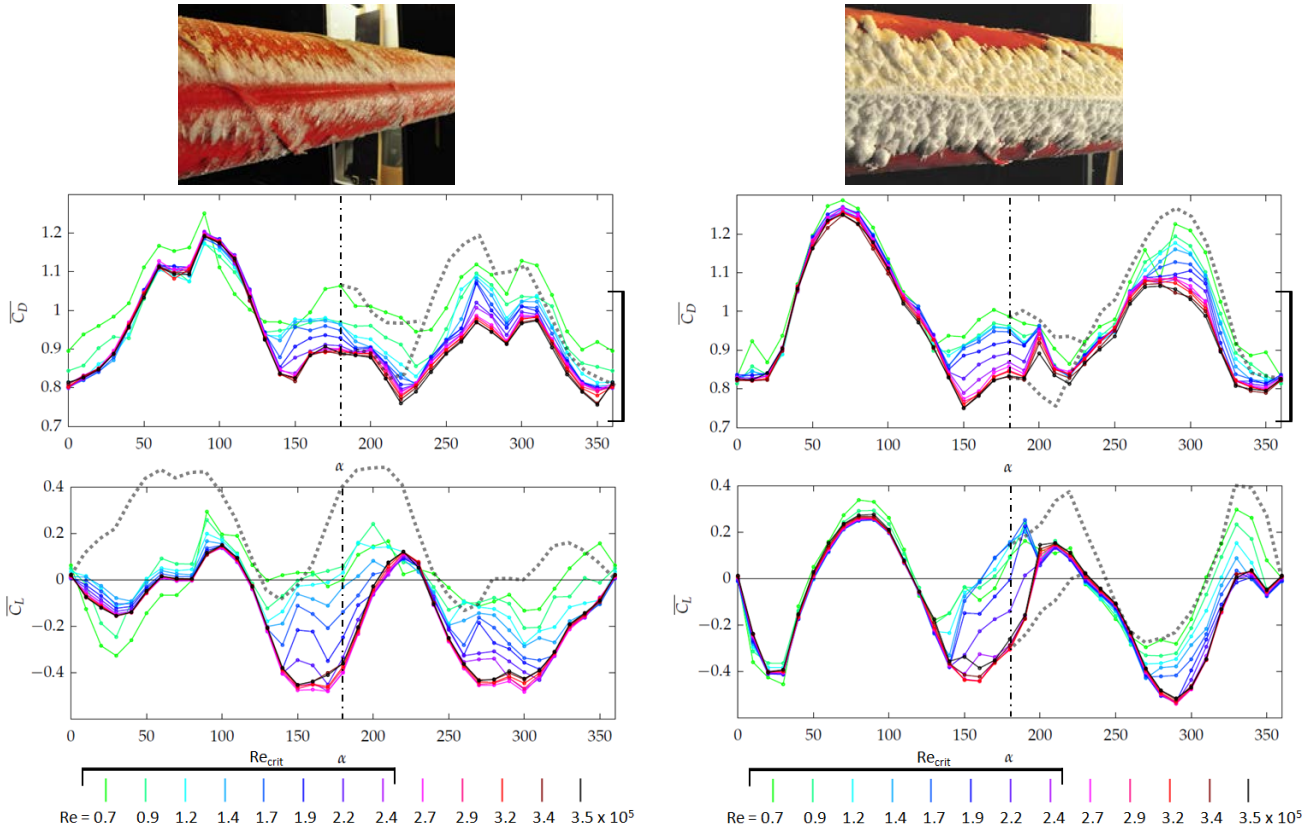

Wet ice accretion (Accretion time: 60min; mean air temperature: -2.2°C; ice mass: 0.46kg/m).

Dry ice accretion (Accretion time: 60min; mean air temperature: -5.1°C; ice mass: 0.49kg/m).

Figure 5 Drag and lift coefficients of helical fillet cable tube.

For wet ice (Figure 5, left) the drag force coefficient is reasonably symmetric around $\alpha = 180°$. Similar to the observation on the plain cable C_D is fairly Reynolds number independent up until 130°. Hereafter, the ice layer enters the wake flow and the cable assumes an aerodynamic behaviour closer to dry cable conditions. The symmetry of the drag force is influenced by the irregularity of the ice layer. This is in particular reflected by the increased level of Reynolds dependency for relative flow direction above 180°. The wet ice layer covers a larger part of the cable tube surface hence influencing the airflow along the tube surface even if the main part of the ice is in the wake flow zone. For this reason the drag coefficient reaches only for some specific angles the low drag level of the dry cable. When the ice layer is near the separation point, i.e. around 90° or 270°, the drag coefficient peaks and exceeds the level of the dry cable up to 15%. Comparing the lift force coefficient curve with its antisymmetric image indicates a very low level of ice layer symmetry. Both curves show a certain resemblance to each other but differ significantly in magnitude.

As observed on the standard plain cable tube the dry ice accretion (Figure 5, right) is more concentrated around the stagnation line compared to wet ice. Both drag and lift coefficient curves indicate a reasonable symmetry allowing for some irregularity. The influence of the ice layer on the drag coefficient magnitude is higher than observed from wet ice accretion. For ice layer positions near flow separation (around 90° or 270°) C_D peaks 1.28, approximately 20% above the maximum drag of the dry cable tube. According to Figure 2 (left) the dry cable exhibits a wide critical range. On the iced cable this dependency appears for relative flow direction placing the ice layer in the wake flow zone of the cable tube ($130° < \alpha < 230°$). The symmetry of the drag curve is influenced by the natural irregularity of the ice layer and by the change of surface roughness throughout the test as discussed for the standard plain cable. The influence of the surface roughness change seems to be smaller on the helical fillet tube than on the plain cable. The fillets define at discrete positions the location of flow separation hence 'damping' the Reynolds number dependency. As discussed above the lift coefficient curve shows a reasonable antisymmetry. The variation of C_L with Reynolds number seems to follow the pattern observed for C_D.

Pattern-Indented Cable

A main feature in the aerodynamic performance of the pattern-indented cable is the low drag coefficient almost constant in the supercritical range starting at a relatively low Reynolds number (Figure 2, left). The C_D range of the dry cable over the Reynolds range applied in this study is indicated to the right in upper graphs In Figure 6. As it appears, the drag coefficients of the wet iced cable stay inside the dry cable drag range but reach only for few relative flow directions the characteristic low drag level. However, the pattern-indented cable tube exhibits even with wet ice a very low Reynolds dependency of the drag force for all tested relative flow directions. This behaviour distinguishes the pattern-indented cable clearly from the standard plain and helical fillet cable. The increased ice mass on the underside of the cable tube (e.g. icicles, shown in the photograph of Figure 6, left) creates some irregularity and asymmetry in the ice layer leading to a limited symmetry of the drag curve. The lift force curve shows for some flow directions a certain variation at low Reynolds numbers. Antisymmetric resemblance is limited and characterised by a difference of lift force coefficients as seen in case HW.

The dry ice layer (Figure 6, right) changes the drag force of the pattern-indented cable stronger than observed for wet ice. The drag coefficients exceed the dry cable values by about 15% for flow directions where the ice layer is near the flow separation point. The effect of ice layer and wake flow and the change of surface roughness on the drag force are similar to the dry ice accretion on the other cable types. Still, main characteristic is the very low dependency on the Reynolds number for all

investigated angles α. The lift force coefficient curve indicates a high irregularity but is, apart from lower airspeeds, Reynolds number independent.

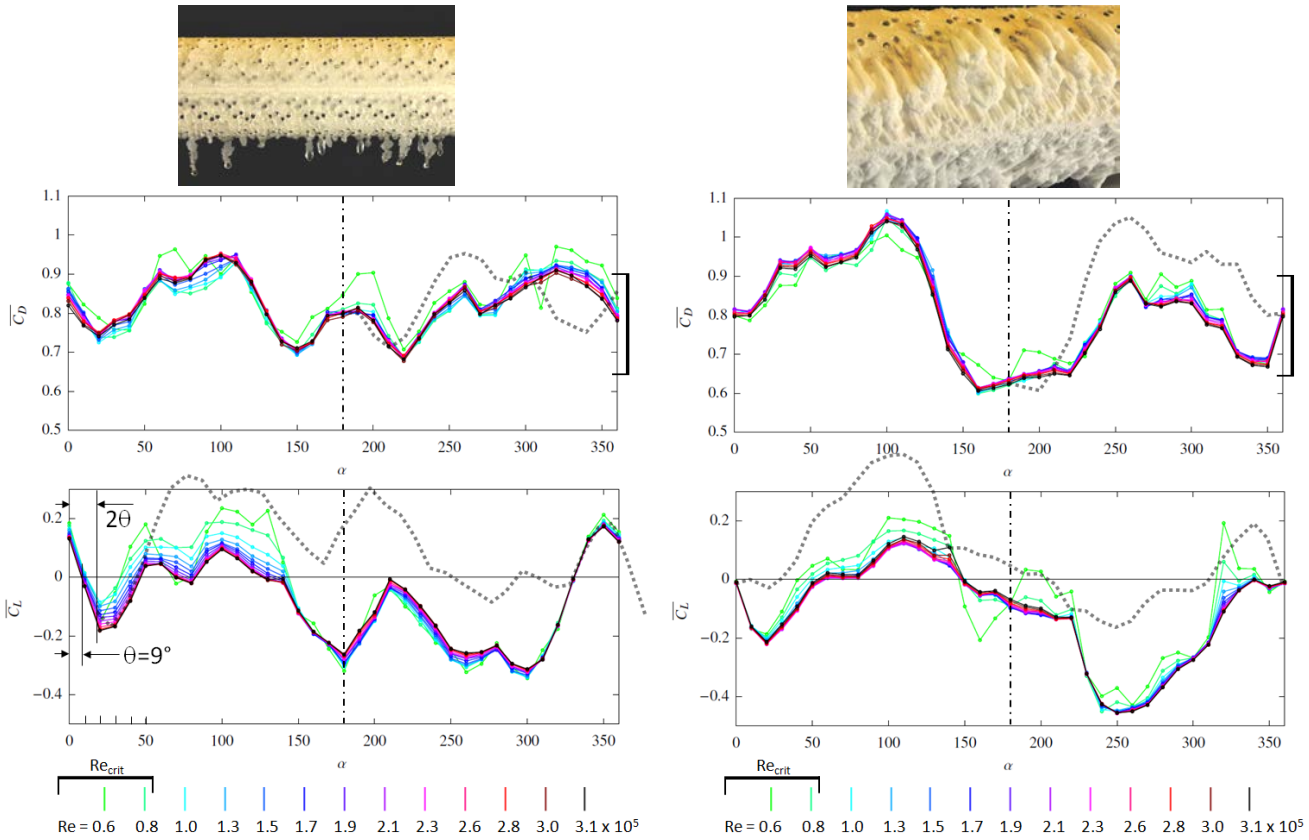

Wet ice accretion (Accretion time: 60min; mean air temperature: -1.8°C; ice mass: 0.53kg/m).

Dry ice accretion (Accretion time: 60min; mean air temperature: -5.3°C; ice mass: 0.6kg/m).

Figure 6 Drag and lift coefficients of pattern-indented cable tube.

CONCLUSIONS

The influence of icing on bridge cable aerodynamics was investigated on three different original full-scale samples of bridge cable cover tubes (standard plain, helical fillet and pattern-indented) for two different types of ice accretion (wet and dry). The tests were performed in specially built wind tunnel facility allowing for simulating in-cloud icing conditions.

- *Wet ice*: the ice layer consists mainly of glaze ice exhibiting a noticeable asymmetry with increased ice mass on the underside of the cable due to gravity.

- *Dry ice*: consisting of rime ice apparently symmetric around stagnation line during accretion phase. Spray dust creates small ice flakes on the rear side of the cable tube surface.

With respect to the influence of the ice layer on aerodynamic performance of the three cable types following main conclusion can be drawn:

- The standard plain cable is most affected by ice accretion with respect to sensibility of drag to Reynolds number, to the magnitude of lift coefficient and to the sensibility of both force coefficients to surface roughness.

- Both helical fillet and pattern-indented cable are less susceptible to changes of the cable surface and ice accretion where the pattern-indented is least affected.

- The pattern-indented cable seems to cope best with the effect of ice accretion. For comparable icing conditions the pattern-indented cable has lower overall drag and lift coefficients compared to standard plain and helical fillet cable.

A more detailed description of the conducted study has been presented on the International Workshop on Atmospheric Icing of Structures, 2013 [8].

REFERENCES

[1] K. Kleissl and C.T. Georgakis, 2012, *Comparison of the aerodynamics of bridge cables with helical fillets and a pattern-indented surface*, Journal of Wind Engineering and Industrial Aerodynamics, vol.104-106, pp.166-175

[2] G. Matteoni and C.T. Georgakis, 2012, *Effects of bridge cable surface roughness and cross-sectional distortion on aerodynamic force coefficients*, Journal of Wind Engineering and Industrial Aerodynamics, Vol.104-106, pp.176-187

[3] C.T. Georgakis, H.H. Koss and F. Ricciardelli, 2009, *Design Specifications for a Novel Climatic Wind Tunnel for the Testing of Structural Cables*. Proceedings 8th International Symposium on Cable Dynamics, Paris, France

[4] H.H. Koss and M.S.M. Lund, 2013, *Experimental Investigation of Aerodynamic Instability of Iced Bridge Sections*, In: 6th European and African Conference on Wind Engineering, Robinson College, Cambridge, UK.

[5] C. Demartino, H.H Koss and F. Ricciardelli, 2013, *Experimental study of the effect of icing on the aerodynamics of circular cylinders – Part I: Cross flow*. In: 6th European and African Conference on Wind Engineering, Robinson College, Cambridge, UK.

[6] C. Demartino, C.T. Georgakis and F. Ricciardelli, 2013, *Experimental study of the effect of icing on the aerodynamics of circular cylinders – Part II: Inclined flow*. In: 6th European and African Conference on Wind Engineering, Robinson College, Cambridge, UK.

[7] H.H. Koss, H. Gjelstrup, C.T. Georgakis, 2012, *Experimental study of ice accretion on circular cylinders at moderate low temperature*., Journal of Wind Engineering and Industrial Aerodynamics, Vol.104-106, pp.540-546.

[8] H.H. Koss, J.F. Henningsen, I. Olsen, 2013, *Influence of Icing on Bridge Cable Aerodynamics*, In: 15th International Workshop on Atmospheric Icing of Structures, St. John's, Newfoundland and Labrador, Canada.